Biophysical Journal
Article

Biophysical Society

Mechanical Properties of Chondrocytes Estimated from Different Models of Micropipette Aspiration

Yongsheng Li,[1] Yueqin Li,[2,3] Quanyou Zhang,[4] Lili Wang,[4] Meiqing Guo,[1] Xiaogang Wu,[4] Yuan Guo,[4] Jing Chen,[4,*] and Weiyi Chen[4,*]

[1]Institute of Applied Mechanics, College of Mechanical and Vehicle Engineering, Taiyuan University of Technology, Taiyuan, China; [2]Shanxi Dayi Hospital, Taiyuan, China; [3]Shanxi Academy of Medical Sciences, Taiyuan, China; and [4]Institute of Biomedical Engineering, College of Biomedical Engineering, Taiyuan University of Technology, Taiyuan, China

ABSTRACT In this study, two viscoelastic creep expressions for the aspirated length of individual solid-like cells undergoing micropipette aspiration (MPA) were derived based on our previous studies wherein the cell size relative to the micropipette and the cell compressibility were taken into account. Next, three mechanical models of MPA, the half-space model (HSM), incompressible sphere model (ICSM), and compressible sphere model (CSM), were employed to fit the MPA data of chondrocytes. The results indicated that the elastic moduli and viscoelastic parameters of chondrocytes for the ICSM and CSM exhibited significantly higher values than those from the HSM ($p < 0.001$) because of the considerations of the geometric parameter (ξ) and the compressibility of the cell (ν). For the normal chondrocytes, the elastic moduli obtained from the ICSM and CSM ($\nu = 0.3$) were 47.4 and 78.9% higher than those from the HSM. In the viscoelasticity, the parameters k_1, k_2, and μ for the ICSM were respectively increased by 37.8, 37.9, and 39.0% compared to those from the HSM, whereas for the CSM ($\nu = 0.3$), the above parameters were 135, 314, and 257% higher compared to those from the HSM. And with the increase of ξ and ν, the above mechanical parameters decreased. Furthermore, the thresholds of ξ varying with ν were obtained for the given values of relative errors caused by the HSM in the elastic and viscoelastic parameters. The above findings obviously indicated that the geometric parameter of MPA and the Poisson's ratio of a cell have marked influences on the determination of cellular mechanical parameters by MPA and thus should be considered in the pursuit of more accurate investigations of the mechanical properties of cells.

INTRODUCTION

The mechanical properties of cells were found to be closely related to many important biological behaviors of cells, including adhesion, migration, differentiation, and deformation (1–4). The mechanical properties of cells, such as stiffness, nonlinearity, anisotropy, and characteristics of the cytoskeleton and organelles, have been extensively studied in the past decades, providing insight into the biological characteristics of cells (5). For example, the stiffness of a chondrocyte with respect to that of the surrounding extracellular matrix will affect its mechanical responses (6), which may in turn modulate its protein synthesis (7). Additionally, connections are also established between the diseased state of human cells and their altered cellular mechanical properties, such as in malaria (8), asthma (9), arthritis (10), and even cancer (11). Therefore, evaluating the mechanical properties of cells may potentially lead to the development of novel mechanical diagnostic methods for some of these diseases (12).

In the past decades, a variety of techniques have been developed to estimate the mechanical properties of single cells, including unconfined compression (13), atomic force microscopy (AFM) (14), micropipette aspiration (MPA) (15), magnetic twisting cytometry (16), and optical trapping (17). MPA is one of the pioneering techniques in cell mechanics and continues to be widely used (18–20). Accurate quantification of the mechanical properties of living cells requires the combined use of experimental techniques and theoretical models. In particular, for the MPA of solid-like cells (cartilage cells, endothelial cells, etc.), a common method is treating the cell as an incompressible elastic or viscoelastic semi-infinite body (21,22) (i.e., the so-called half-space model (HSM)). However, under the premise of linear constitutive relations and small deformations, the HSM is still quite different from the actual situation of MPA in two aspects. First, compared to the inner radius of a micropipette, the cell size is fairly finite and is generally on the same order of magnitude. Second, many studies

Submitted July 30, 2018, and accepted for publication April 18, 2019.

*Correspondence: 819903@163.com or 1165059779@qq.com

Editor: Joseph Zasadzinski.

https://doi.org/10.1016/j.bpj.2019.04.022

have indicated that cells are compressible, with a Poisson's ratio varying from 0.2 to 0.4 (23–25) and even reaching 0.069, as reported by Leipzig and Athanasiou (13) for bovine chondrocytes. Thus, the HSM is inadequate for characterizing the MPA of a spherical cell. A more accurate model is necessary.

Numerous studies have been carried out in the pursuit of the accurate determination of cellular mechanical properties utilizing MPA. Haider and Guilak (26,27) investigated the elastic and viscoelastic responses of cells during MPA by using the boundary element method in which the dimension of the cell, the cell boundary curvature, and the cell-micropipette contact, but not the cell compressibility, were considered. Zhou et al. (28) simulated the MPA of cells by using the standard neo-Hookean solid model in which three relationships were derived that neglected the cell compressibility when interpreting the mechanical parameters of cells. Baaijens et al. (29) determined the mechanical properties of chondrocytes by using the finite element method and concluded that the cell diameter should be greater than three times the inner pipette diameter to reduce the effect of cell curvature when employing the HSM, wherein a compressible neo-Hookean model characterizing the hyperelasticity was adopted. Bidhendi and Korhonen (25) simulated the MPA of single cells by using neo-Hookean viscohyperelastic incompressible and compressible models to study the creep behavior of cells, particularly the effect of compressibility. These previous studies demonstrated that the aspirated cell length during MPA is closely related to the compressibility of the cell and the relative dimension of the cell to the micropipette. Nevertheless, a general expression of the aspirated length considering the influences of the size and compressibility of the cell simultaneously was not given in the above studies, which would make it inconvenient or impossible to accurately analyze the mechanical properties of each type of solid-like cell by MPA. Spector et al. (30) investigated the deformations of cochlear outer hair cell in the MPA in which the cell was modeled as an elastic and compressible cylindrical shell and derived the analytical solution of the aspirated length. Furthermore, on the basis of microstructural observation, a more accurate model, an orthotropic cylindrical shell was developed to characterize the outer hair cell (31), and then an approximate formula for the length of the tongue into the pipette during MPA was derived, which led to an analytical expression for the stiffness parameter measured in the MPA in terms of Young's moduli and Poisson's ratios of the cell. However, the works above may be more suitable for the elongated cells rather than the spherical ones, and all only focused on the elastic responses of cell. In our previous study (32), an approximate elastic formula of the aspirated length of a cell was obtained through theoretical and finite element analysis in which both the cell size and compressibility were considered. Further, the above approximate formula was verified by the aspiration of foam silicone rubber spheres with different diameters and mechanical properties by a self-developed aspiration system (33). The formula could be used as a reference in the accurate determination of the elastic parameters of solid-like cells by MPA.

Many studies have indicated that cells are essentially viscoelastic (i.e., the force and deformation of cells are time dependent) (34,35). Therefore, the goal of this study was first to derive the viscoelastic expressions for the aspiration response of a cell based on the approximate elastic formula obtained in our previous studies (32,33) in which the size and compressibility of the cell were taken into account. Second, combined with the experimental data of MPA for rabbit chondrocytes, differences in mechanical properties estimated by different mechanical models were evaluated, with a focus on the influences of the relative dimension between the cell and the micropipette and the Poisson's ratio of the cell on the determination of mechanical parameters. This work was performed to provide some general formulas as a reference for the viscoelastic analysis of solid-like cells from MPA data. It should be pointed out that the aim of this study was to investigate the changes in mechanical parameters caused by different mechanical models, whereas the variations in cellular mechanical properties caused by different physiological and medical backgrounds would not be discussed in detail.

MATERIALS AND METHODS

HSM

For the MPA of the spherical solid-like cells, such as chondrocytes and endothelial cells, the HSM is widely employed to evaluate the mechanical properties of cells (18–23), wherein the size and compressibility of the cell were neglected as mentioned above. Although it was mentioned in the Introduction that the adoption of HSM required the cell diameter to be larger than three times of the inner micropipette diameter, many studies have employed this model regardless of the geometric condition (18–20). In the range of linear elasticity and small deformation, the analytical relationship between the aspirated length (L_h, the subscript h indicates the HSM) and the negative pressure (Δp) (as shown in Fig. 1 *a*), can be expressed as follows (21):

$$L_h = \frac{3a\Delta p}{2\pi E}\Phi(\eta), \tag{1}$$

where a is the inner radius of the micropipette, E is the elastic modulus of the cell, and $\Phi(\eta)$ is the wall function of the micropipette.

Furthermore, based on Eq. 1, a viscoelastic creep expression for the aspirated length was derived by Sato et al. (22), wherein the cell was treated as an incompressible standard linear solid (SLS), as shown in Fig. 1 *b*. The aspirated length can be expressed as follows:

$$L_h(t) = \frac{a\Delta p}{\pi k_1}\Phi(\eta)\left[1+\left(\frac{k_1}{k_1+k_2}-1\right)\exp\left(-\frac{t}{\tau}\right)\right]H(t). \tag{2}$$

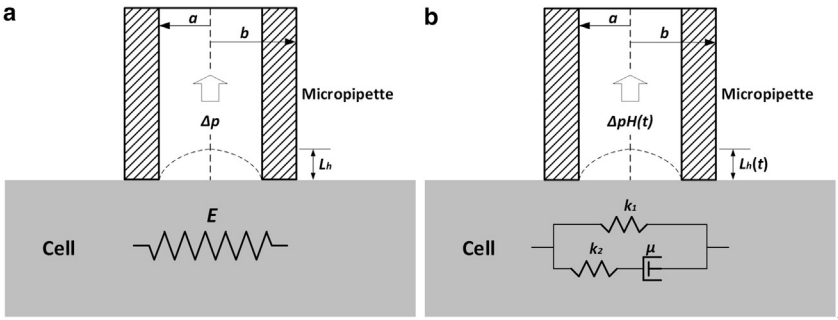

FIGURE 1 Schematic representations of the half-space model (HSM) for the MPA of a single cell. (*a*) The linear elastic medium is shown. (*b*) The SLS model is shown.

Here, L_h (t) is the aspiration length of the cell at time t; k_1, k_2, and μ, the three viscoelastic parameters of the SLS model, were determined by nonlinear regression analysis of the MPA data. τ is the relaxation time constant of a deformation under constant load (defined as $\tau = \mu(k_1 + k_2)/(k_1k_2)$), and $H(t)$ is the Heaviside function. As is well known, Eq. 2 is widely applied in the viscoelastic analysis of cells (18–20,35–38).

SM

Considering the differences between the HSM and the actual situation of MPA, a sphere model (SM) was employed in which the relative dimension of cell to micropipette and the compressibility of the cell were considered, as shown in Fig. 2 *a*. In the conditions of linear elasticity and small deformation, an approximate elastic formula for the aspirated length of the cell was obtained through theoretical analysis and numerical methods (32) and was expressed as follows:

$$L_s = A\left(1+\frac{B}{\xi^C}\right)\left(1-\nu^2\right)\frac{3a\Delta p}{2\pi E}\Phi(\eta). \tag{3}$$

Here, L_s denotes the aspirated length of the cell in the SM (the subscript s represents the SM), ξ is the relative dimension of the radius of cell (R) to the inner radius of micropipette (a), and ν is the Poisson's ratio of the cell. A, B, and C are dimensionless parameters independent of Δp and E. According to our previous study (32), the above three parameters were set to 1.33, 0.76, and 0.93, respectively. It should be noted that Eq. 3 has been validated via the aspiration experiments of foam silicone rubber spheres performed in our self-developed aspiration system (33), which provided further support for the reliability of the approximate formula.

Furthermore, assuming the cell behaves as a homogeneous isotropic and compressible SLS medium, as shown in Fig. 2 *b*, the governing equations of the viscoelastic problem in the absence of a body force are as follows:

$$\left.\begin{aligned}
&\sigma_{ij,j} = 0 \quad \text{(a)}\\
&\varepsilon_{ij} = \frac{1}{2}\left(u_{i,j}+u_{j,i}\right)\text{(b)}\\
&\sigma_{ij} = \sigma\delta_{ij}+S_{ij}\ ,\ \varepsilon_{ij} = e\delta_{ij}+e_{ij}\\
&\sigma = 3Ke\ ,\ \sigma = \frac{1}{3}\sigma_{kk},\ e = \frac{1}{3}\varepsilon_{kk}\\
&S_{ij}+p_1\dot{S}_{ij} = q_0e_{ij}+q_1\dot{e}_{ij}
\end{aligned}\right\}\text{(c)} \quad \text{in } \Omega. \tag{4}$$

Here, σ_{ij}, ε_{ij}, and δ_{ij} represent the stress tensor, strain tensor, and the Kronecker delta, respectively. $u_{i,j}$ and $u_{j,i}$ are the relative displacement tensors. σ and e are the mean of the principle stresses and principle strains, respectively. S_{ij} and e_{ij} denote the stress deviator tensor and strain deviator tensor, respectively. K is the bulk modulus, and p_1, q_0, and q_1 are constants relevant to material parameters k_1, k_2, and μ. The term (a) of Eq. 4 is the equilibrium equation, and (b) is the compatibility relations in the condition of infinitesimal strains. We assumed that the volume change of the cell obeyed the law of elasticity and that the shape change followed the SLS model (39), as shown in term (c) of Eq. 4. The symbol "˙" denotes the derivative of tensors with respect to time. The parameters K, p_1, q_0, and q_1 are defined as follows:

$$K = \frac{E}{3(1-2\nu)} \text{ and} \tag{5}$$

$$p_1 = \frac{\mu}{k_2}, q_0 = k_1, q_1 = \frac{\mu(k_1+k_2)}{k_2}. \tag{6}$$

Because of the symmetry of the model, it can be simplified as a plane problem. In the polar coordinate system, the boundary conditions are

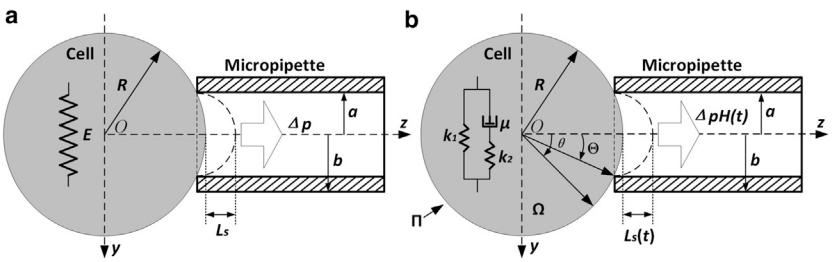

FIGURE 2 Sphere model of the MPA of a single cell employing different constitutive relations. (*a*) The linear elastic model is shown. (*b*) The SLS model (Ω is the space representing the cell and Π denotes the boundary of Ω) is shown.

$$\left.\begin{array}{c}\tau_{r\theta}(R,\theta,t) = 0 \text{ for } t \geq 0 \\ \sigma_r(R,\theta,t) = \Delta p H(t) \text{ for } -\Theta < \theta < \Theta \text{ and } t \geq 0 \; \Theta = \arcsin\dfrac{a}{R} \\ = 0 \;\; for \; \Theta < \theta < 2\pi - \Theta \text{ and } t \geq 0 \\ u_r(R,\theta,t) = 0 \;\; for \; \theta = \pm\Theta \text{ and } t \geq 0 \end{array}\right\} \text{on } \Pi. \tag{7}$$

The initial conditions are

$$u = \dot{u} = 0 \text{ in } \Omega \text{ for } t = 0. \tag{8}$$

Because of the premise of linearity of the constitutive relations and geometry, the solution for the aspirated length $L_s(t)$ for the above viscoelastic problem can be derived by the corresponding principle of elasticity to viscoelasticity based on the solution of the corresponding elastic problem (i.e., Eq. 3) (39,40). Next, two cases will be discussed.

Incompressible sphere model

By letting ν be 0.5, Eq. 3 is reduced to

$$L_s = \left(1 + \frac{B}{\xi^C}\right) \frac{3a\Delta p}{2\pi E} \Phi(\eta). \tag{9}$$

Then, in Eq. 4, we have

$$\left.\begin{array}{c} e = 0 \\ K = \infty \end{array}\right\}. \tag{10}$$

Thus, term (c) of Eq. 4 can be rewritten as

$$\left.\begin{array}{c} \sigma_{ij} = -p\delta_{ij} + S_{ij} \\ S_{ij} + p_1\dot{S}_{ij} = q_0 e_{ij} + q_1 \dot{e}_{ij} \end{array}\right\}, \tag{11}$$

where p is the hydrostatic stress, which is defined as the mean of the three principle stresses. The Laplace transformation of Eq. 11 is

$$\left.\begin{array}{c} \overline{\sigma}_{ij} = -\overline{p}\delta_{ij} + \overline{S}_{ij} \\ (1 + sp_1)\overline{S}_{ij} = (q_0 + sq_1)\overline{e}_{ij} \end{array}\right\}. \tag{12}$$

By substituting the second formula of Eq. 12 into the first, the Laplace transformation of the constitutive equation for the incompressible SLS can be rewritten as

$$\overline{\sigma}_{ij} = -\overline{p}\delta_{ij} + \frac{q_0 + sq_1}{1 + sp_1}\overline{e}_{ij}. \tag{13}$$

The corresponding constitutive equation of elasticity for the incompressible case is expressed as

$$\sigma_{ij} = -p\delta_{ij} + 2\mu\varepsilon_{ij}, \tag{14}$$

where μ is the Lamé constant of an elastic body. Comparing Eqs. 13 and 14, we have

$$\underset{\sim}{\overline{\mu}} = \frac{q_0 + sq_1}{2(1 + sp_1)}. \tag{15}$$

Here, $\underset{\sim}{\overline{\mu}}$ is the corresponding value of the elastic constant μ in the Laplace domain for the viscoelastic constitutive relation. Moreover, in the condition of incompressibility, the elastic modulus can be expressed as

$$E = 3\mu. \tag{16}$$

By substituting Eq. 16 into Eq. 9 and replacing μ and Δp with $\underset{\sim}{\overline{\mu}}$ and $\Delta\overline{p}(s)$, the Laplace transformation of the viscoelastic solution of the aspirated length, $L_s(t)$, can be derived as follows:

$$\overline{L}_s(s) = \left(1 + \frac{B}{\xi^C}\right) \frac{a\Delta\overline{p}(s)}{2\pi\underset{\sim}{\overline{\mu}}} \Phi(\eta). \tag{17}$$

Generally, the negative pressure Δp during MPA is applied by step type, that is,

$$\Delta p = \Delta p H(t) = \left\{\begin{array}{ll} \Delta p & t \geq 0 \\ 0 & t < 0 \end{array}\right., \tag{18}$$

where $H(t)$ is the Heaviside function. Thus, we can obtain

$$\Delta\overline{p}(s) = \frac{\Delta p}{s}. \tag{19}$$

By substituting Eqs. 15 and 19 into Eq. 17, it can be rewritten as

$$\overline{L}_s(s) = \left(1 + \frac{B}{\xi^C}\right) \frac{a\Delta p\Phi(\eta)}{\pi} \times \frac{1 + sp_1}{s(q_0 + sq_1)}. \tag{20}$$

Then, the viscoelastic solution of the incompressible sphere model (ICSM) is obtained as follows from the inverse Laplace transformation of Eq. 20:

$$\begin{aligned} L_s(t) = &\left(1 + \frac{B}{\xi^C}\right) \frac{a\Delta p}{\pi k_1} \Phi(\eta) \\ &\times \left[1 + \left(\frac{k_1}{k_1 + k_2} - 1\right)\exp\left(-\frac{t}{\tau}\right)\right] H(t). \end{aligned} \tag{21}$$

The parameters in Eq. 21 are the same as those in Eqs. 2 and 3. Obviously, Eqs. 2 and 21 have the same form, except for the correction coefficient $(1 + B/\xi^C)$.

Compressible sphere model

When a cell is considered compressible, the viscoelastic constitutive relations are (39)

$$\left\{\begin{array}{c} \sigma = 3Ke \\ S_{ij} + p_1\dot{S}_{ij} = q_0 e_{ij} + q_1 \dot{e}_{ij} \end{array}\right. . \tag{22}$$

From the Laplace transformation of term (c) of Eq. 4, we have

$$\overline{\sigma}_{ij} = \overline{\sigma}\delta_{ij} + \overline{S}_{ij} = 3K\overline{e}\delta_{ij} + \frac{q_0 + sq_1}{1 + sp_1}\overline{e}_{ij}. \tag{23}$$

Noting that

$$\overline{e} = \frac{1}{3}\overline{\varepsilon}_{kk} \text{ and } \overline{e}_{ij} = \overline{\varepsilon}_{ij} - \overline{e}\delta_{ij}, \tag{24}$$

thence the Eq. 23 can be further written as

$$\overline{\sigma}_{ij} = \left[K - \frac{q_0 + sq_1}{3(1 + sp_1)}\right]\overline{\varepsilon}_{kk}\delta_{ij} + \frac{q_0 + sq_1}{1 + sp_1}\overline{\varepsilon}_{ij}. \tag{25}$$

The elastic constitutive relation of the compressible sphere model (CSM) is given by

$$\sigma_{ij} = \lambda\delta_{ij}\varepsilon_{kk} + 2\mu\varepsilon_{ij}, \tag{26}$$

where λ is another Lamé constant of an elastic body. Comparing Eqs. 25 and 26, the following correspondences can be obtained:

$$\begin{cases} \underset{\sim}{\overline{\lambda}} = K - \dfrac{q_0 + sq_1}{3(1 + sp_1)} \\ \underset{\sim}{\overline{\mu}} = \dfrac{q_0 + sq_1}{2(1 + sp_1)} \end{cases}. \tag{27}$$

By substituting Eq. 27 into Eq. 3, the viscoelastic solution of the aspirated length for the CSM in the Laplace domain can be expressed as follows:

$$\overline{L}_s = \left[A\left(1 + \frac{B}{\xi^C}\right)\frac{3a\Delta p}{4\pi}\Phi(\eta)\right] \times \left[\frac{2(1 + sp_1)}{s(q_0 + sq_1)} - \frac{3K(1 + sp_1) - (q_0 + sq_1)}{6K(1 + sp_1) + (q_0 + sq_1)} \times \frac{2(1 + sp_1)}{s(q_0 + sq_1)}\right]. \tag{28}$$

Then, from the inverse Laplace transformation of Eq. 28, the aspirated length $L_s(t)$ for the CSM is derived as

$$L_s(t) = \left[A\left(1 + \frac{B}{\xi^C}\right)\frac{3a\Delta p}{2\pi}\Phi(\eta)\right] \times \left[\frac{3K + 2q_0}{q_0(6K + q_0)} + \frac{p_1q_0 - q_1}{2q_0q_1}\exp\left(-\frac{q_0}{q_1}t\right) + \frac{3(p_1q_0 - q_1)}{2(6K + q_0)(6Kp_1 + q_1)}\exp\left(-\frac{6K + q_0}{6Kp_1 + q_1}t\right)\right]H(t). \tag{29}$$

Here, K, p_1, q_0, and q_1 are the undetermined parameters described for Eqs. 5 and 6. It is noted that K should be calculated first from Eq. 5, where E is determined by fitting the MPA data obtained from the elastic responses to Eq. 3 and ν is generally given in the range from 0.2 to 0.4. Then, the viscoelastic parameters k_1, k_2, and μ can be determined by fitting the creep curve for MPA to Eq. 29. It can be found that when $\nu \to 0.5$ (i.e., $K \to \infty$), Eq. 29 will degenerate to Eq. 21.

MPA of chondrocytes

The normal and osteoarthritis (OA) chondrocytes were harvested from the articular cartilage of male New Zealand white rabbits under the same feeding conditions ($n = 16$; 3–5 months old; 1.8–2.5 kg body weight; 8 per group). An animal model of OA was experimentally induced in the OA group by anterior cruciate ligament transection, and the same operation was performed on the normal group without anterior cruciate ligament transection. Rabbits were allowed to move freely in the cages until their sacrifice at 15 weeks postsurgery. The study was undertaken with the approval of the ethics committee of the Taiyuan University of Technology. Rabbits' articular cartilages were inspected at two levels: macroscopic and histological in all left knees. The cartilage degeneration of the joint was evaluated using a modification of Mankin's histologic classification (grade 0–6). If the mean grade value was less than or equal to 1.5, the cartilage was classified as normal, and a mean grade value greater than 1.5 was classified as OA. The cartilage was removed from the bone and digested with 0.4% pronase then with 0.025% collagenase type II at 37°C until a single-cell suspension was obtained. Isolated primary cells were suspended in culture medium with Dulbecco's Modified Eagle Medium (Nissui, Tokyo, Japan), Nutrient Mixture F-12 (Solarbio, Beijing, China) with 10% fetal bovine serum and 1% penicillin, and used for the MPA test immediately.

The MPA of chondrocytes was generally similar to that described previously (10,23), as shown in Fig. 3. Approximately 1 mL of chondrocyte suspension was loaded into a small chamber. The tip of the micropipette was made to approach the surface of a spherical chondrocyte. Before the aspiration experiments, the diameter of the cell and the inner diameter of the micropipette were first recorded. In the initial state of the experiment, a negative pressure of ~0.01 kPa was applied to the chondrocyte, and the mouth of pipette was sealed against the cell. Then, a step negative pressure of 0.02 kPa amplitude was applied, which caused an instantaneous elastic deformation of the cell. Each pressure was maintained for 10 s until the cell reached a steady state, and the aspirated length of the cell was recorded along with the corresponding negative pressure. The maximal pressure was controlled to be less than 0.25 kPa. Subsequently, the negative pressure was fixed to a desired value (ranging from 0.3 to 0.4 kPa) for 200 s, which caused a time-dependent aspiration of a portion of the chondrocyte. All experiments were performed at 37°C and controlled humidity (custom-built equipment) within 2 h.

Statistical analysis

The data obtained in this study were presented as the mean ± SD. Statistical analyses were conducted using the software SPSS (version 17.0; IBM,

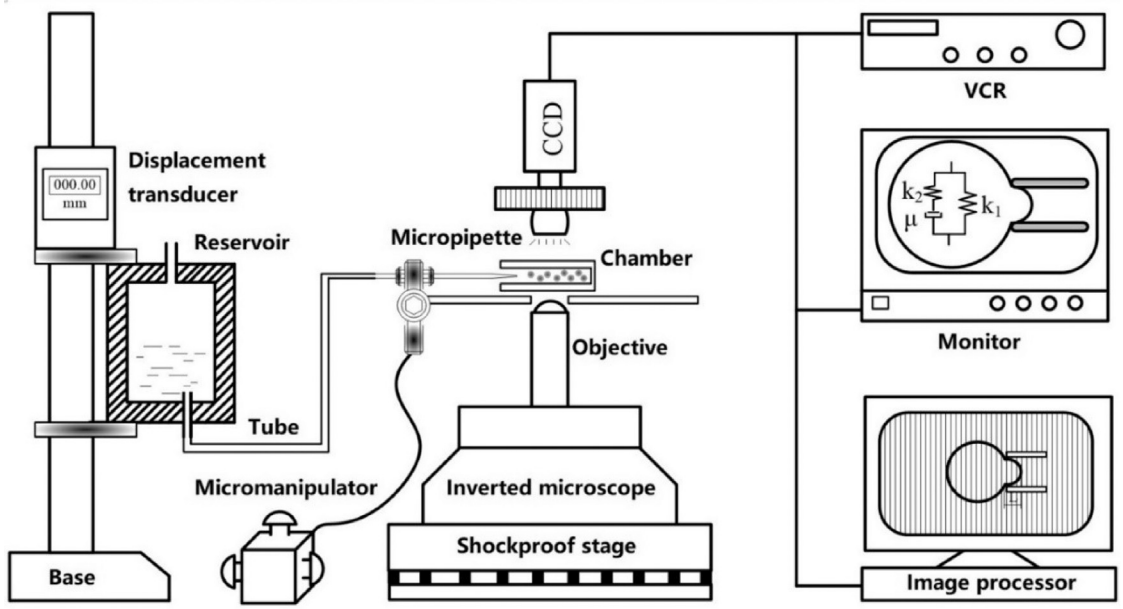

FIGURE 3 Schematic diagram of MPA (55).

Armonk, NY). Because of the approximate normal distribution of data, an independent *t*-test was used to examine the differences between the groups (normal and OA). The statistical significance between the models (HSM, ICSM, and CSM) was estimated by two-factor analysis of variance. Differences were considered statistically significant at $p < 0.05$.

RESULTS

Mechanical parameters from different models

The chondrocytes showed an instantaneous elastic behavior under the action of step negative pressure in which the aspirated length was approximately linearly related to the pressure. When the pressure was fixed at a certain value (~0.35 kPa), the typical creep behavior of a viscoelastic solid was exhibited by the chondrocytes (i.e., an instantaneous jump followed by a decreasing slope until equilibrium was reached), as described in previous studies (10,36). For the elastic response, Eqs. 1, 3, and 9 were used to fit the experimental data to determine the elastic modulus E and bulk modulus K of the cell (for the CSM, ν was taken as 0.2, 0.3, and 0.4). The viscoelastic creep response was fitted by Eqs. 2, 21, and 29 to obtain the parameters k_1, k_2, and μ, where the parameter K of Eq. 29 was set to the above determined values. The wall function $\Phi(\eta)$ was adopted as 2.05 during the whole process of fitting. The fitting curves of MPA data for the normal and OA chondrocytes using the three models (HSM, ICSM, and CSM) are shown as Fig. 4.

Table 1 presents the mechanical parameters of chondrocytes derived from the three models. For the normal group, the HSM yielded an $E = 0.57 \pm 0.43$ kPa, a $k_1 = 0.37 \pm 0.07$ kPa, a $k_2 = 0.29 \pm 0.04$ kPa, and a $\mu = 6.36 \pm 1.12$ kPa·s. However, because of the consideration of cell size, the ICSM generated higher parameters as $E = 0.84 \pm 0.66$ kPa, $k_1 = 0.51 \pm 0.09$ kPa, $k_2 = 0.40 \pm 0.06$ kPa, and $\mu = 8.84 \pm 1.52$ kPa·s. For the CSM ($\nu = 0.3$), wherein the compressibility of cell was further taken into account, the much higher parameters were produced as $E = 1.02 \pm 0.79$ kPa, $k_1 = 0.87 \pm 0.05$ kPa, $k_2 = 1.20 \pm 0.38$ kPa, and $\mu = 22.72 \pm 2.93$ kPa·s, except for a finite bulk modulus K as equals 0.85 ± 0.66 kPa. For the OA group, the effects of the model were similar to

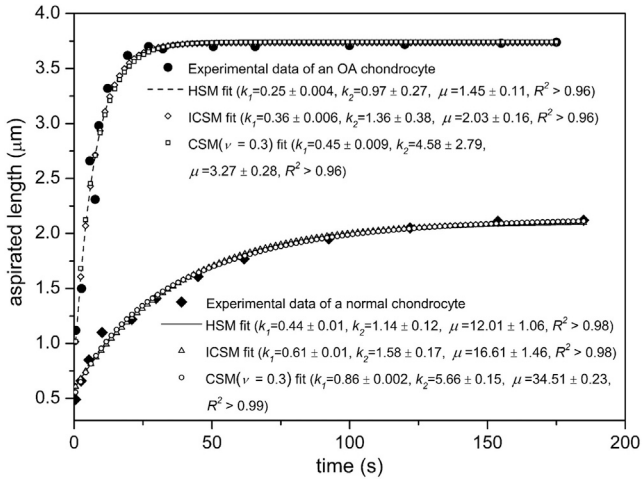

FIGURE 4 Viscoelastic responses for a normal chondrocyte and an OA chondrocyte during the MPA fitted by three models. For the normal chondrocyte, the parameters ξ and a were 2.09 and 3.66 μm; for the OA chondrocyte, they were respectively 1.99 and 3.63 μm. The aspiration pressure was 0.38 kPa for both cells. The units of viscoelastic parameters k_1, k_2, and μ are kPa, kPa and kPa·s, respectively.

TABLE 1 Elastic and Viscoelastic Parameters of Normal and OA Chondrocytes Obtained from Different Models

	Normal ($n = 47$)					OA ($n = 50$)				
	Elastic		Viscoelastic			Elastic		Viscoelastic		
Model	E (kPa)	K (kPa)	k_1 (kPa)	k_2 (kPa)	μ (kPa·s)	E (kPa)	K (kPa)	k_1 (kPa)	k_2 (kPa)	μ (kPa·s)
HSM	0.57 ± 0.43	$+\infty$	0.37 ± 0.07	0.29 ± 0.04	6.36 ± 1.12	0.54 ± 0.40[a]	$+\infty$	0.26 ± 0.09[b]	0.20 ± 0.09[b]	0.39 ± 0.14[b]
ICSM	0.84 ± 0.66[c]	$+\infty$	0.51 ± 0.09[c]	0.40 ± 0.06[c]	8.84 ± 1.52[c]	0.76 ± 0.55[a]	$+\infty$	0.37 ± 0.13[b]	0.29 ± 0.13[b]	0.56 ± 0.19[b]
CSM0.4	0.94 ± 0.73[c,d]	1.57 ± 1.22	0.69 ± 0.02[c,d]	0.79 ± 0.10[c,d]	15.82 ± 1.81[c,d]	0.84 ± 0.62[a]	1.41 ± 1.03[a]	0.46 ± 0.08[b]	0.53 ± 0.13[b]	0.93 ± 0.18[b]
CSM0.3	1.02 ± 0.79[c,d]	0.85 ± 0.66	0.87 ± 0.05[c,d]	1.20 ± 0.38[c,d]	22.72 ± 2.93[c,d]	0.91 ± 0.67[a]	0.76 ± 0.56[a]	0.62 ± 0.05[b]	0.82 ± 0.16[b]	1.37 ± 0.27[b]
CSM0.2	1.07 ± 0.84[c,d]	0.60 ± 0.47	1.03 ± 0.13[c,d]	1.37 ± 0.13[c,d]	27.32 ± 3.85[c,d]	0.96 ± 0.70[a]	0.54 ± 0.39[a]	0.71 ± 0.10[b]	0.92 ± 0.18[b]	1.57 ± 0.19[b]

[a] $p > 0.05$ compared to the normal group.
[b] $p < 0.001$ compared to the normal group.
[c] $p < 0.001$ compared to the HSM.
[d] $p < 0.001$ compared to the ICSM.

those of the normal group, except that the parameters were lower than those of the normal group in the same model.

Comparisons of groups in different models

As shown in Fig. 5 *a*, the elastic modulus of OA chondrocytes from each model was slightly lower than that of the normal group, and no significant difference was observed between the two groups ($p > 0.05$). The above results were all consistent with the findings by Jones et al. (23) for human chondrocytes obtained by means of the HSM. For the viscoelasticity, the three parameters of OA chondrocytes for each model were all significantly lower than those of normal chondrocytes ($p < 0.001$), which was contrary to the results of previous study by Trickey et al. (10,35). With regard to the HSM, the k_1, k_2, and μ of the OA group decreased by 27.9, 31.0, and 93.9%, respectively, compared to those of the normal group; for the ICSM, the above values were 27.5, 27.5, and 93.7%, respectively (Fig. 5, *b–d*). For the CSM, with $\nu = 0.3$ as an example, the above values were 28.7, 31.7, and 94.0%, respectively (Fig. 5, *b–d*). Obviously, the effects of models on the relative differences of mechanical parameters between the normal and OA chondrocytes were roughly the same.

Comparisons of models

Elasticity

It can also be found from Table 1 that the differences in elastic parameters caused by the use of different mechanical models were significant for each group. The elastic moduli estimated by the ICSM and CSM were larger than those of the HSM. For the normal group, the elastic modulus from the ICSM was 47.4% higher than that of the HSM ($p < 0.001$; Fig. 6 *a*). For the CSM, the percentage increase in E over the value for the HSM was 87.7, 78.9, and 64.9% when the Poisson's ratio was set to 0.2, 0.3, and 0.4, respectively, as illustrated in Fig. 6 *a*. Thus, the dimension of the cell relative to the micropipette (ξ) and the Poisson's ratio (ν) have a marked effect on the determination of E and should be considered. It can also be observed that the elastic modulus changes little when the Poisson's ratio varies from 0.2 to 0.4. The E for $\nu = 0.4$ was only 12% lower than that for $\nu = 0.2$. However, the effect of ν on the bulk modulus K was significant, that is, K for $\nu = 0.4$ was 162% higher than that for $\nu = 0.2$ (Table 1). Therefore, when employing the CSM, although the value of ν has little effect on the determination of the elastic modulus, this choice can lead to a drastic change in K, which may greatly affect the subsequent viscoelastic analysis.

Viscoelasticity

Additionally, as can be observed from Table 1, the viscoelastic parameters of cells determined from the different

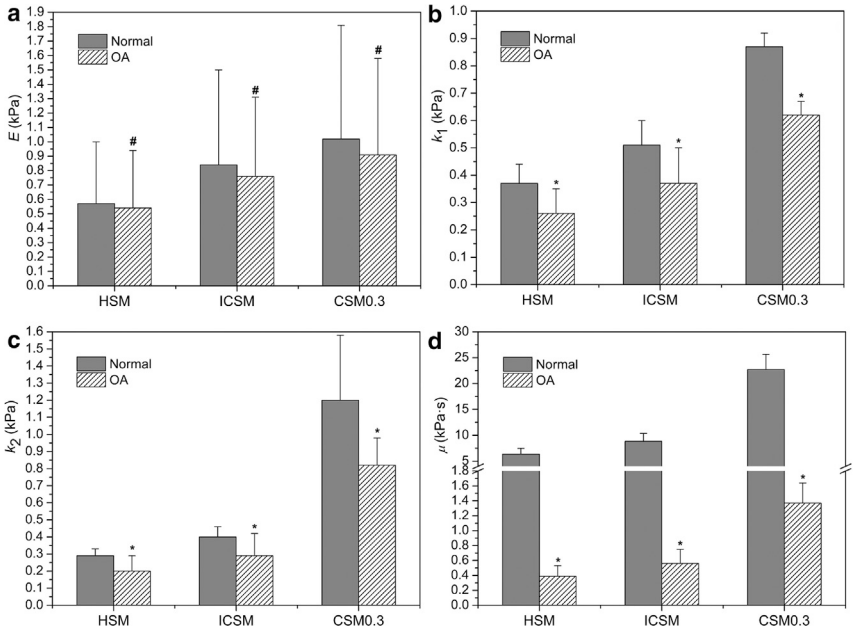

FIGURE 5 Comparisons between the normal ($n = 47$) and OA ($n = 50$) groups in terms of the mechanical parameters estimated from different models. Elastic modulus (E) and viscoelastic parameters (k_1, k_2, and μ) were respectively shown in (a)–(d). $^{\#}p > 0.05$ and $^{*}p < 0.001$ as compared to the normal group.

models were significantly different regardless of the group. For the normal group, the parameters for the ICSM and CSM were significantly larger than those of the HSM ($p < 0.001$). The k_1, k_2, and μ for the ICSM were 37.8, 37.9, and 39.0% higher, respectively, than those for the HSM (Fig. 6, *b–d*). The above differences were caused by the consideration of the relative size of the cell and the micropipette. For the CSM, the viscoelastic parameters decreased with the increase of ν. When $\nu = 0.3$, k_1, k_2, and μ increased by 71.0, 200, and 157%, respectively, relative to those of the ICSM ($p < 0.001$; Fig. 6, *b–d*). For the cases of $\nu = 0.2$ and $\nu = 0.4$, the above parameters were respectively 102, 243, and 209% and 35.3, 97.5, and 79% higher than those of the ICSM. The above results indicated that the value of Poisson's ratio had a significant influence on the determination of the viscoelastic parameters. If we consider the combined effects of ξ and ν on the viscoelastic parameters, for the normal group, k_1, k_2, and μ at $\nu = 0.3$

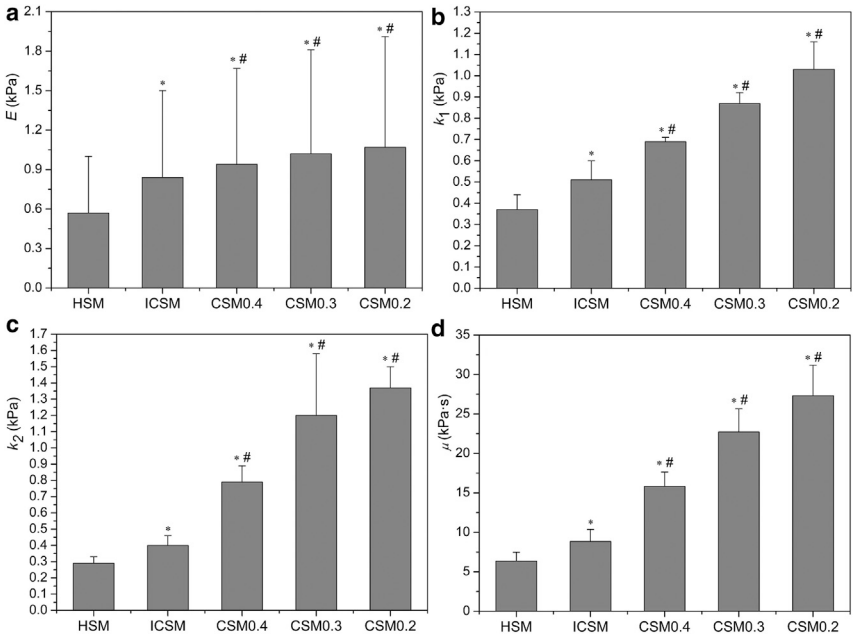

FIGURE 6 Comparisons of the mechanical parameters between the different models for the normal group ($n = 47$). Elastic modulus (E) and viscoelastic parameters (k_1, k_2, and μ) were shown in (a)–(d), respectively. $^{*}p < 0.001$ as compared to HSM and $^{\#}p < 0.001$ as compared to ICSM.

were 135, 314, and 257% higher, respectively, than those for the HSM (Fig. 6, *b–d*). Thus, it can be concluded that the influences of the parameter (ξ) characterizing the dimension of the cell relative to the micropipette and Poisson's ratio (ν) on the estimation of the cellular viscoelastic parameters were very significant and should be taken into consideration for an accurate determination of mechanical parameters of cells by MPA.

Effects of models on the OA group

For the OA group, the percentage increases in E for the ICSM and CSM ($\nu = 0.3$) over that for the HSM were 40.7 and 68.5%, respectively, and the viscoelastic parameters k_1, k_2, and μ for the ICSM and CSM ($\nu = 0.3$) were respectively 42.3, 45, and 43.6% and 138, 310, and 251% higher than those for the HSM. The above results were close to those of the normal group.

Predictions for the relative errors of mechanical parameters caused by HSM

Because of the consideration of geometric parameter (ξ) and compressibility of cell (ν) in the SM, we believe that the mechanical parameters obtained from this model are more accurate (closer to the actual values) than those obtained from the HSM. According to Eqs. 1 and 3, we can derive the elastic moduli of the cell from the HSM and SM as follows:

$$\begin{cases} E_h = \dfrac{3a\Delta p\Phi(\eta)}{2\pi L} \\ E_s = A\left(1+\dfrac{B}{\xi^C}\right)\left(1-\nu^2\right)\dfrac{3a\Delta p\Phi(\eta)}{2\pi L} \end{cases}. \tag{30}$$

Here, L is the aspiration length of the cell during MPA, and the subscripts h and s represent the HSM and SM, respectively. Defining e as the relative change of elastic moduli (or relative error) between the HSM and SM, we have

$$\begin{aligned} e &= \left|\frac{E_h - E_s}{E_s}\right| \times 100\% \\ &= \left[1 - A^{-1}\left(1+\frac{B}{\xi^C}\right)^{-1}\left(1-\nu^2\right)^{-1}\right] \times 100\% \end{aligned}. \tag{31}$$

The thresholds of ξ corresponding to different Poisson's ratios can be obtained for some given values of e, as shown in Fig. 7.

As can be seen when ν is 0.3, to make the e less than 30%, ξ needs to be at least 5.0. When ν equals 0.5 (ICSM), ξ is ~3.3 to make the e reach 20%. However, ξ is rarely larger than 5.0 in general MPA experiments; thus, the relative error of the modulus will exceed 30%. It can also be found from

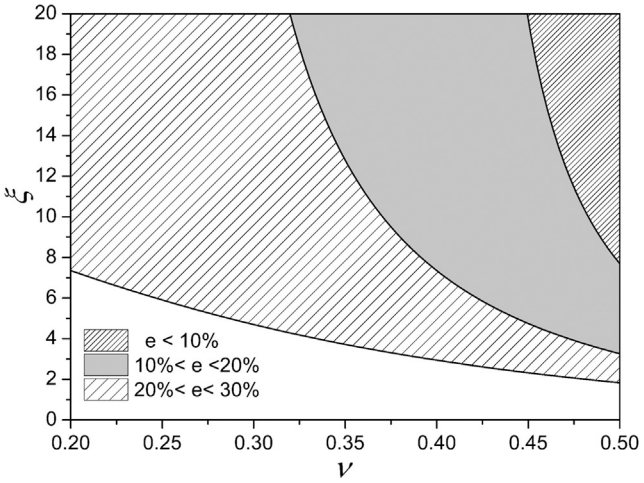

FIGURE 7 Thresholds of ξ varying with ν when e was 10, 20, and 30%, respectively.

Eq. 31 that the above results are independent of cell types, so they are applicable to other spherical solid-like cells.

For the viscoelastic parameters, another parameter V_R was introduced to represent the relative errors of parameters between the HSM and SM, which is expressed as

$$V_R = \left|\frac{V_h - V_s}{V_s}\right| \times 100\%. \tag{32}$$

Here, V_h and V_s represent the viscoelastic parameters from the HSM and SM, and the subscripts h and s denote the HSM and SM, respectively. From Eqs. 2 and 21, we can find that the V_R of the three parameters (k_1, k_2, and μ) between the HSM and ICSM are identical and equal to $[B/(B + \xi^C)]\times 100\%$. As can be seen from Fig. 8 *a*, V_R decreases with the increase of ξ. When ξ is 3, V_R is nearly 22%. If the ξ is larger than 8.0, the relative error will be reduced to less than 10%. Similar to the e, the above results also apply to other types of cells. For the CSM, the viscoelastic parameters are related to both ξ and K (Eq. 29), and K can be expressed as follows according to Eqs. 5 and 30:

$$K = \frac{A\left(1+\frac{B}{\xi^C}\right)\left(1-\nu^2\right)}{3(1-2\nu)}E_h. \tag{33}$$

To investigate the effects of ξ and ν, E_h should be given first. The viscoelastic parameters of a typical chondrocyte varying with ξ and ν were obtained, as shown in Fig. 8, *b–d*. It can be observed that the parameters decrease with the increase of ξ and ν. When ν tends to 0.5, the parameters tend to those of the ICSM. When the ξ exceeds 10, each parameter changes very little. For a certain Poisson's ratio ($\nu = 0.3$), when ξ is 3, the V_R of k_1, k_2, and μ are 47.1, 70.8, and 68.2%, respectively. When ξ equals 5 and

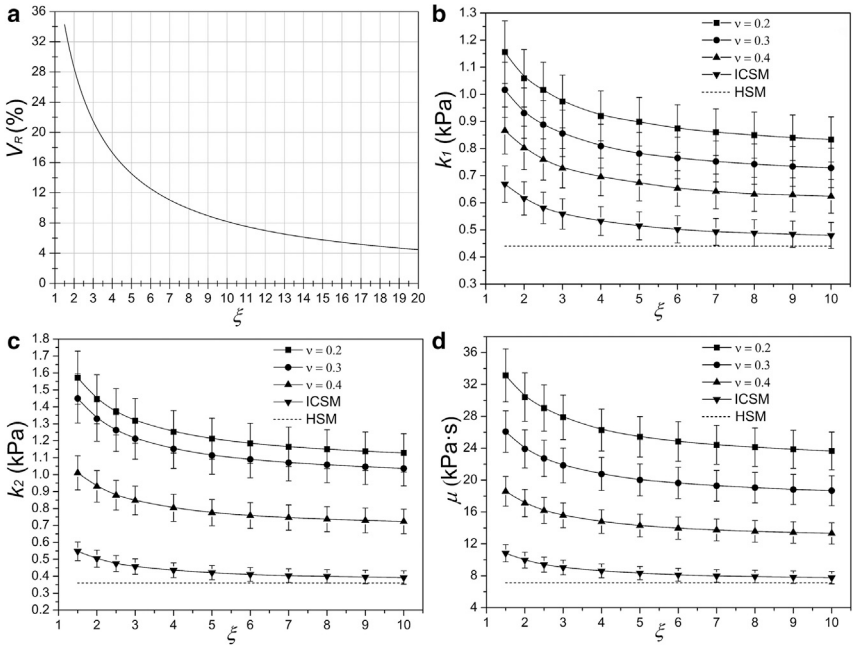

FIGURE 8 Effects of ξ and ν on the viscoelastic parameters. (*a*) The relative errors of viscoelastic parameters between the HSM and ICSM as a function of ξ are shown. (*b*)–(*d*) exhibit the variations of three viscoelastic parameters (k_1, k_2, and μ) with ξ at different Poisson's ratios, in which the pipette inner diameter (*a*), negative pressure (Δp), and E_h of the chondrocyte were 3.56 μm, 0.4, and 0.6 kPa, respectively.

10, the above values are 42.3, 68.8, and 65% and 38.4, 66.0, and 63.2%, respectively. For a given ξ ($\xi = 3$), when ν is 0.2, the V_R of k_1, k_2, and μ are 53.6, 73.3, and 75.0%, respectively. When ν is taken as 0.3 and 0.4, the above errors are 47.7, 71.1, and 68.2% and 38.4, 58.8, and 54.8%, respectively. Thus, the V_R also decreases with the increase of ξ and ν.

DISCUSSION

Two general creep characterizations of MPA considering the dimension of a cell relative to the micropipette and the cell compressibility were obtained based on our previous studies on the corresponding elastic behaviors. Then, combined with the MPA data of chondrocytes, comparisons between different models demonstrated that the geometric parameter (ξ) and the Poisson's ratio (ν) can affect the determination of mechanical parameters significantly and should not be neglected in an accurate analysis of the mechanical properties of cells.

Comparisons to other testing methods (AFM, unconfined compression, or cytoindentation), as shown in Table 2, revealed that the elastic moduli of chondrocytes determined by means of different approaches were on the same order of magnitude, and the results of this study were generally lower than the corresponding values obtained by other methods. This finding can be attributed to several factors, the most obvious being differences in the testing methodologies. As a matter of fact, the cell is a highly heterogeneous structure in which the cortical shell envelops the liquid cytoplasm with many organelles inside. Recent study has shown that the stiffness of cells mostly comes from the cortex of cells, and the cytoplasm is a weak elastic gel with a stiffness three orders lower than that of the cortex (41). It is also important to note that the nucleus accounts for a significant part of the cell responses (42). Experimentation using

TABLE 2 Elastic and Viscoelastic Properties of Normal Chondrocytes Measured by Different Methods

	AFM		Unconfined Compression/Cytoindentation			MPA (Current Study)		
	$\nu = 0.5$[a]	$\nu = 0.38$[b]	$\nu = 0.5$[c]	$\nu = 0.26$[d]	$\nu = 0.5$[e]	ICSM	CSM0.38	CSM0.26
E (kPa)	1.4 ± 1.1	0.94	2.55 ± 0.85	–	1.10 ± 0.48	0.84 ± 0.66	0.99 ± 0.87	1.12 ± 0.75
E_0 (kPa)	0.91	0.42	2.47 ± 0.85	1.06 ± 0.82	8.00 ± 4.41	0.91 ± 0.14	1.75 ± 0.35	2.25 ± 0.44
E_∞ (kPa)	0.45 ± 0.44	0.24	1.48 ± 0.35	0.78 ± 0.58	1.09 ± 0.54	0.51 ± 0.09	0.75 ± 0.06	0.93 ± 0.11
μ (kPa·s)	4.46	0.88	1.92 ± 1.80	4.08 ± 7.20	1.50 ± 0.92	8.84 ± 1.52	17.26 ± 2.52	25.43 ± 4.25

[a]Human ($n = 46$). E_0 and μ were calculated from the data provided by (53).
[b]Data were obtained by averaging the values from superficial and middle/deep zones (34) (porcine).
[c]Bovine (13) ($n = 15$).
[d]Bovine (50) ($n = 24$).
[e]Bovine (54) ($n = 16$).

micropipette techniques has shown that isolated nuclei from chondrocytes are three to four times stiffer than the cell (43), and other experiments using AFM have demonstrated similar results in adherent endothelial cells (44). Thus, whether using the MPA, AFM, or unconfined compression, the derived mechanical properties of the whole cell mainly reflect the stiffness of the cortex and nucleus of the cell. However, relative to the influence of cortex and nucleus on cell response during MPA, we consider that they have a greater effect on the cellular response in unconfined compression, for the unconfined compression exposes the entire cell to compressive force, whereas micropipette experiments use suction to expose a portion of the cell membrane to tensile forces. Additionally, cells from different animals and different joint locations were compared, which could also cause the significantly different variations in mechanical properties (45,46). Lastly, differences in mechanical properties could arise from the fact that the other methods (AFM, unconfined compression, or cytoindentation) were conducted on cells that were adhered to a substratum, whereas MPA tests suspended cells. The process of cellular adhesion is known to involve the formation of focal adhesion complexes in conjunction with cytoskeleton remodeling (47). This adhesion process has been demonstrated to produce an overall stiffening of the cell (48,49).

With regard to the viscoelasticity, the parameters of this study (ICSM) were close to those from AFM ($\nu = 0.5$), except that the apparent viscosity coefficient μ differed (Table 2). The instantaneous modulus E_0 (defined as $k_1 + k_2$) and the equilibrium modulus E_∞ (defined as k_1) from this study were significantly lower than those determined by unconfined compression or cytoindentation, which was also probably the result of the stiffer nuclei mentioned above. The CSM0.38 and CSM0.26 of this study also yielded similar E_0 and E_∞ values as those from AFM and unconfined compression. However, in the above comparisons, the μ obtained from the MPA of this study was higher than that from AFM, unconfined compression, or cytoindentation. The authors believe that for this difference, the most obvious factor, in addition to the reasons stated above, was the different treatment of the Poisson's ratio when switching from elasticity to viscoelasticity. In this study, during the derivation of the viscoelastic expression for MPA from the elastic formula, the Poisson's ratio was considered a function of time, similar to the elastic modulus. Therefore, the viscoelastic formula does not contain ν explicitly (39) but does contain the bulk modulus K, which was markedly influenced by ν, as stated previously (Table 1). Thus, as ν increases, K will increase dramatically, which will in turn cause large changes in the three viscoelastic parameters, especially μ. In contrast, the viscoelastic expression characterizing the response of the creep cytoindentation of chondrocytes given by Shieh and Athanasiou (50),

$$d(t) = \frac{h_0\sigma}{(1+\nu)E_\infty}\left[1+\left(\frac{\tau_\varepsilon}{\tau_\sigma}-1\right)\exp\left(-\frac{t}{\tau_\sigma}\right)\right]H(t), \quad (34)$$

and the viscoelastic formula describing the stress relaxation of AFM for chondrocytes derived by Darling et al. (34),

$$F(t) = \frac{4R^{1/2}\delta_0^{3/2}E_\infty}{3(1-\nu)}\left[1+\left(\frac{\tau_\sigma}{\tau_\varepsilon}-1\right)\exp\left(-\frac{t}{\tau_\varepsilon}\right)\right]H(t), \quad (35)$$

explicitly contained the Poisson's ratio (i.e., ν was considered time independent), similar to the geometric parameter ξ in this study. However, the authors considered that it is reasonable to treat ν as a time-dependent variable in the derivation. Similar to E, ν is also an intrinsic parameter of an elastic body, so these values should be treated equally in the transformation from elasticity to viscoelasticity. Simply, because of the difficulties in the accurate determination of the Poisson's ratio of cells, cells are generally considered incompressible or given a value of ν in advance, and the main attention is focused on the elastic modulus, which is closely related to the cellular stiffness. From the above two formulas, it can be found that the viscoelastic parameters decrease as ν increases, which is consistent with the prediction of this study. The difference is that the influences of the Poisson's ratio on the viscoelastic parameters can be easily determined directly from the above two formulas, but not from Eq. 29 of this study. For example, if the Poisson's ratio varies from 0.5 to 0.2, the viscoelastic parameters all increase by 25% for Eq. 34 and 60% for Eq. 35, which are much smaller than the corresponding results obtained in this study (Table 1). On the whole, with the exception of μ, the mechanical parameters of chondrocytes obtained by MPA in this study are roughly on the same order of magnitude as those obtained with other methods. In terms of the mechanical model of MPA in the current work, the cell size and compressibility were considered simultaneously, and the elastic formula has been validated by experiments. Therefore, the authors consider that the mechanical parameters of chondrocytes obtained in this study provide an important reference for relevant studies involving the mechanical properties of chondrocytes.

In the results, it was mentioned that for the OA group, the relative changes of mechanical parameters caused by different models were close to those of the normal group. It was attributed to two factors, ξ and E_h. According to Eqs. 31 and 32, we can find that the relative differences of the elastic modulus between the HSM and SM and the viscoelastic parameters between the HSM and ICSM were determined by ξ and ν. Whereas, for the viscoelastic parameters from the CSM, in addition to ξ, they were also related to the bulk modulus (K) as expressed by Eq. 33. Therefore, under the same Poisson's ratio, the relative changes of

parameters caused by different models were determined by both ξ and E_h. In the current study, the differences in ξ (2.01 $\pm$ 0.27 and 2.19 $\pm$ 0.24 for normal and OA groups, respectively) and E_h (0.57 $\pm$ 0.43 kPa and 0.54 $\pm$ 0.40 kPa for normal and OA groups, respectively, as presented in Table 1) between the two groups were slight, so the relative changes of mechanical parameters caused by different models were very close for the normal and OA chondrocytes. Consequently, the relative differences of mechanical parameters between the two groups were also almost identical in the different models as illustrated in Fig. 5. However, for other types of cells or diseases, the effects of models would be quite different if there was a large difference between the two groups of cells (normal and diseased) in ξ or E_h.

In addition, contrary to this study, a previous study on viscoelasticity of human chondrocytes indicated that OA chondrocytes exhibit higher k_1, k_2, and μ than the normal group (10). However, the chondrocytes utilized in that study were harvested from different patients with end-stage OA undergoing joint replacement surgery or undergoing amputation or surgical correction of tumors or bone fractures. Obviously, the factors of age, sex, OA degree, etc. of these patients were uncertain. These may lead to the different mechanical properties of chondrocytes.

There are also some significant limitations in the current study. One of the most obvious is the assumption that the cell is a homogeneous and isotropic viscoelastic material. This assumption can greatly simplify the model. Actually, considering the underlying structure, a chondrocyte is a complex unit containing various organelles and a cytoskeleton. The cytoskeleton has been assumed to be the source of the solid-like elastic response of the cell, whereas the viscoelastic component of the cell is not as well understood and may be attributed to fluid-solid interactions, fluid viscosity, or the nature of the cytoskeleton itself. Therefore, in some sense, a mixture theory or poroelastic models may be more suitable for describing the deformation behavior of a single chondrocyte. Another significant limitation is the assumption of linear constitutive relations and of a small deformation during the whole process of MPA, including the elastic and viscoelastic response. Only with this premise, the viscoelastic creep response of the aspirated length of a cell during MPA could be obtained from the correspondence principle based on the elastic formula derived in our previous study. In a similar way, the creep response of indentation depth in the cytoindentation (50) and the analytical solution of relaxation of the applied force exerted on the chondrocytes by AFM (34) were derived. In fact, the MPA of cells is a process involving a finite deformation (28,29,51), even under a small negative pressure. In some cases, pure strains slightly greater than 30% were observed. Thus, the assumption of a small deformation in the current study may lead to significant errors. However, some studies demonstrated that the infinitesimal strain assumption may still be accurate for a viscoelastic HSM of MPA (which generates cellular strains greater than 30%). Moreover, the previous finite element simulation indicated that for the CSM ($a = 3$ μm, $\xi = 7$, $E = 500$ Pa, $\nu = 0.499$, and $\Delta p = 100$ Pa), the total elastic strain in the contact area between the cell and micropipette exceeded 50% (51), which was far beyond the scope of the small deformation ($\varepsilon < 5\%$). However, the simulation results also indicated that the aspirated length can still maintain a satisfactory linear relationship with the negative pressure within the range of 150 Pa (51).

Moreover, the micropipette was modeled as a standard hollow cylinder with a sharp corner in this study; thus, the effect of the pipette fillet radius on the aspiration response was not considered. However, according to the simulation results of Zhou et al. (28), the above effect would be significant for the situations of larger ξ. Finally, the viscoelastic expressions obtained in this study for the SM of MPA of cells were strictly applicable to cells with a spherical or approximately spherical morphology (such as suspended chondrocytes, endothelial cells, or fibroblasts). For irregularly shaped cells or adherent cells, the formulas cannot be applied directly. If the effect of the geometric parameter (the ratio of the inner radius of the micropipette to the characteristic size of the cell) on the aspirated length can be properly corrected (it can refer to the approach given by Boudou et al. (52)), the resulting formulas might also be used to describe the response of cells during MPA.

CONCLUSIONS

Based on our previous studies on the elastic response of a single cell undergoing MPA, two viscoelastic creep expressions for the aspirated length of a cell considering the size and compressibility of cells were obtained in this work. To our knowledge, this is the first study to provide analytical expressions characterizing the creep behavior of a cell that considers the combined influences of the cell geometry and compressibility during MPA. Furthermore, the MPA data of chondrocytes from normal and OA articular cartilages of rabbits were fitted by the aspiration formulas of the HSM, ICSM and CSM, and the elastic and viscoelastic parameters of each model were obtained. Comparisons between the models demonstrated that the mechanical parameters (E, k_1, k_2, and μ) of chondrocytes obtained from the ICSM and CSM were significantly higher than from those of the HSM and increased with the decrease of geometric parameter (ξ) and Poisson's ratio (ν). Moreover, the relative errors of mechanical parameters caused by the HSM were introduced, and the thresholds of ξ varying with ν were obtained for the given values of errors. These results indicated that the effects of the relative dimension between the cell and micropipette and the Poisson's ratio of cell were remarkable and should be taken into consideration. Additionally, as a result of the close values in ξ and E_h of

the two groups, the choice of models had little influence in charactering the relative differences of mechanical properties between normal and OA chondrocytes. However, for other types of cells or diseases, the effects of models may differ significantly in different ξ and E_h. The authors consider that the viscoelastic formulas obtained in this study may provide a more accurate method for the determination of the mechanical properties of individual solid-like cells and could be used as a reference in relevant studies of cell mechanics.

SUPPORTING MATERIAL

Supporting Material can be found online at https://doi.org/10.1016/j.bpj.2019.04.022.

AUTHOR CONTRIBUTIONS

W.C. conceived the original idea. Y.L. and J.C. designed the research, performed the derivation of formulas, and wrote the article. Q.Z. performed the MPA experiments. Y.L., L.W., and M. G. analyzed the data. Y.L., Y.G., and X.W. wrote the article.

ACKNOWLEDGMENTS

The authors thank Professor Zhongwei Guan of University of Liverpool and Dr. Xiaona Li of Taiyuan University of Technology for their valuable suggestions in this study.

Supports from the National Natural Science Foundation of China (grant nos. 11632013, 11572213, 11702184, and 11472185), the Natural Science Foundation of the Shanxi province of China (no. 201801D121019), the Science and Technology Innovation Project of the Universities of Shanxi province (no. 173230099-S), and the International Cooperation Project Foundation of the Shanxi province of China (no. 201603D421037) are acknowledged.

REFERENCES

1. Arnaout, M. A., S. L. Goodman, and J. P. Xiong. 2007. Structure and mechanics of integrin-based cell adhesion. *Curr. Opin. Cell Biol.* 19:495–507.
2. Lange, J. R., and B. Fabry. 2013. Cell and tissue mechanics in cell migration. *Exp. Cell Res.* 319:2418–2423.
3. Lautenschläger, F., S. Paschke, …, J. Guck. 2009. The regulatory role of cell mechanics for migration of differentiating myeloid cells. *Proc. Natl. Acad. Sci. USA.* 106:15696–15701.
4. Schiffhauer, E. S., and D. N. Robinson. 2017. Mechanochemical signaling directs cell-shape change. *Biophys. J.* 112:207–214.
5. Kirmizis, D., and S. Logothetidis. 2010. Atomic force microscopy probing in the measurement of cell mechanics. *Int. J. Nanomedicine.* 5:137–145.
6. Guilak, F., and V. C. Mow. 2000. The mechanical environment of the chondrocyte: a biphasic finite element model of cell-matrix interactions in articular cartilage. *J. Biomech.* 33:1663–1673.
7. Bachrach, N. M., W. B. Valhmu, …, V. C. Mow. 1995. Changes in proteoglycan synthesis of chondrocytes in articular cartilage are associated with the time-dependent changes in their mechanical environment. *J. Biomech.* 28:1561–1569.
8. Suresh, S., J. Spatz, …, T. Seufferlein. 2005. Connections between single-cell biomechanics and human disease states: gastrointestinal cancer and malaria. *Acta Biomater.* 1:15–30.
9. An, S. S., B. Fabry, …, J. J. Fredberg. 2006. Do biophysical properties of the airway smooth muscle in culture predict airway hyperresponsiveness? *Am. J. Respir. Cell Mol. Biol.* 35:55–64.
10. Trickey, W. R., G. M. Lee, and F. Guilak. 2000. Viscoelastic properties of chondrocytes from normal and osteoarthritic human cartilage. *J. Orthop. Res.* 18:891–898.
11. Guck, J., S. Schinkinger, …, C. Bilby. 2005. Optical deformability as an inherent cell marker for testing malignant transformation and metastatic competence. *Biophys. J.* 88:3689–3698.
12. Lee, G. Y., and C. T. Lim. 2007. Biomechanics approaches to studying human diseases. *Trends Biotechnol.* 25:111–118.
13. Leipzig, N. D., and K. A. Athanasiou. 2005. Unconfined creep compression of chondrocytes. *J. Biomech.* 38:77–85.
14. Roduit, C., S. Sekatski, …, S. Kasas. 2009. Stiffness tomography by atomic force microscopy. *Biophys. J.* 97:674–677.
15. Hochmuth, R. M. 2000. Micropipette aspiration of living cells. *J. Biomech.* 33:15–22.
16. Maksym, G. N., B. Fabry, …, J. J. Fredberg. 2000. Mechanical properties of cultured human airway smooth muscle cells from 0.05 to 0.4 Hz. *J. Appl. Physiol.* 89:1619–1632.
17. Mills, J. P., L. Qie, …, S. Suresh. 2004. Nonlinear elastic and viscoelastic deformation of the human red blood cell with optical tweezers. *Mech. Chem. Biosyst.* 1:169–180.
18. Sliogeryte, K., S. D. Thorpe, …, M. M. Knight. 2016. Differential effects of LifeAct-GFP and actin-GFP on cell mechanics assessed using micropipette aspiration. *J. Biomech.* 49:310–317.
19. Wang, Z., A. K. Wann, …, M. M. Knight. 2016. IFT88 influences chondrocyte actin organization and biomechanics. *Osteoarthritis Cartilage.* 24:544–554.
20. Mohammadkarim, A., M. Tabatabaei, …, M. M. Khani. 2018. Radiation therapy affects the mechanical behavior of human umbilical vein endothelial cells. *J. Mech. Behav. Biomed. Mater.* 85:188–193.
21. Theret, D. P., M. J. Levesque, …, L. T. Wheeler. 1988. The application of a homogeneous half-space model in the analysis of endothelial cell micropipette measurements. *J. Biomech. Eng.* 110:190–199.
22. Sato, M., D. P. Theret, …, R. M. Nerem. 1990. Application of the micropipette technique to the measurement of cultured porcine aortic endothelial cell viscoelastic properties. *J. Biomech. Eng.* 112:263–268.
23. Jones, W. R., H. P. Ting-Beall, …, F. Guilak. 1999. Alterations in the Young's modulus and volumetric properties of chondrocytes isolated from normal and osteoarthritic human cartilage. *J. Biomech.* 32:119–127.
24. Trickey, W. R., F. P. Baaijens, …, F. Guilak. 2006. Determination of the Poisson's ratio of the cell: recovery properties of chondrocytes after release from complete micropipette aspiration. *J. Biomech.* 39:78–87.
25. Bidhendi, A. J., and R. K. Korhonen. 2012. A finite element study of micropipette aspiration of single cells: effect of compressibility. *Comput. Math. Methods Med.* 2012:192618.
26. Haider, M. A., and F. Guilak. 2000. An axisymmetric boundary integral model for incompressible linear viscoelasticity: application to the micropipette aspiration contact problem. *J. Biomech. Eng.* 122:236–244.
27. Haider, M. A., and F. Guilak. 2002. An axisymmetric boundary integral model for assessing elastic cell properties in the micropipette aspiration contact problem. *J. Biomech. Eng.* 124:586–595.
28. Zhou, E. H., C. T. Lim, and S. T. Quek. 2005. Finite element simulation of the micropipette aspiration of a living cell undergoing large viscoelastic deformation. *Mech. Adv. Mater. Struct.* 12:501–512.
29. Baaijens, F. P., W. R. Trickey, …, F. Guilak. 2005. Large deformation finite element analysis of micropipette aspiration to determine the mechanical properties of the chondrocyte. *Ann. Biomed. Eng.* 33:494–501.

30. Spector, A. A., W. E. Brownell, and A. S. Popel. 1996. A model for cochlear outer hair cell deformations in micropipette aspiration experiments: an analytical solution. *Ann. Biomed. Eng.* 24:241–249.

31. Spector, A. A., W. E. Brownell, and A. S. Popel. 1998. Analysis of the micropipet experiment with the anisotropic outer hair cell wall. *J. Acoust. Soc. Am.* 103:1001–1006.

32. Li, Y. S., and W. Y. Chen. 2013. Finite element analysis of micropipette aspiration considering finite size and compressibility of cells. *Sci. China Phys. Mech. Astron.* 56:2208–2215.

33. Li, Y., J. Chen, …, W. Chen. 2018. Experimental verification of the elastic formula for the aspirated length of a single cell considering the size and compressibility of cell during micropipette aspiration. *Ann. Biomed. Eng.* 46:1026–1037.

34. Darling, E. M., S. Zauscher, and F. Guilak. 2006. Viscoelastic properties of zonal articular chondrocytes measured by atomic force microscopy. *Osteoarthritis Cartilage.* 14:571–579.

35. Zhang, Q. Y., X. H. Wang, …, W. Y. Chen. 2008. Characterization of viscoelastic properties of normal and osteoarthritic chondrocytes in experimental rabbit model. *Osteoarthritis Cartilage.* 16:837–840.

36. Sato, M., N. Ohshima, and R. M. Nerem. 1996. Viscoelastic properties of cultured porcine aortic endothelial cells exposed to shear stress. *J. Biomech.* 29:461–467.

37. Guilak, F., G. R. Erickson, and H. P. Ting-Beall. 2002. The effects of osmotic stress on the viscoelastic and physical properties of articular chondrocytes. *Biophys. J.* 82:720–727.

38. Pachenari, M., S. M. Seyedpour, …, H. Hosseinkhani. 2014. Mechanical properties of cancer cytoskeleton depend on actin filaments to microtubules content: investigating different grades of colon cancer cell lines. *J. Biomech.* 47:373–379.

39. Zhou, G. Q., and X. M. Liu. 1996. Theory of Viscoelasticity. Press of University of Science and Technology of China, Hefei, China, In Chinese.

40. Fung, Y. C. 1965. Foundations of Solid Mechanics. Prentice-Hall, Englewood Cliffs, NJ.

41. Guo, M., A. F. Pegoraro, …, D. A. Weitz. 2017. Cell volume change through water efflux impacts cell stiffness and stem cell fate. *Proc. Natl. Acad. Sci. USA.* 114:E8618–E8627.

42. Pajerowski, J. D., K. N. Dahl, …, D. E. Discher. 2007. Physical plasticity of the nucleus in stem cell differentiation. *Proc. Natl. Acad. Sci. USA.* 104:15619–15624.

43. Guilak, F., J. R. Tedrow, and R. Burgkart. 2000. Viscoelastic properties of the cell nucleus. *Biochem. Biophys. Res. Commun.* 269:781–786.

44. Mathur, A. B., G. A. Truskey, and W. M. Reichert. 2000. Atomic force and total internal reflection fluorescence microscopy for the study of force transmission in endothelial cells. *Biophys. J.* 78:1725–1735.

45. Athanasiou, K. A., A. Agarwal, …, M. Clem. 1995. Biomechanical properties of hip cartilage in experimental animal models. *Clin. Orthop. Relat. Res* 254–266.

46. Treppo, S., H. Koepp, …, A. J. Grodzinsky. 2000. Comparison of biomechanical and biochemical properties of cartilage from human knee and ankle pairs. *J. Orthop. Res.* 18:739–748.

47. LeBaron, R. G., and K. A. Athanasiou. 2000. Extracellular matrix cell adhesion peptides: functional applications in orthopedic materials. *Tissue Eng.* 6:85–103.

48. Wang, N., and D. E. Ingber. 1994. Control of cytoskeletal mechanics by extracellular matrix, cell shape, and mechanical tension. *Biophys. J.* 66:2181–2189.

49. Wang, N., and D. E. Ingber. 1995. Probing transmembrane mechanical coupling and cytomechanics using magnetic twisting cytometry. *Biochem. Cell Biol.* 73:327–335.

50. Shieh, A. C., and K. A. Athanasiou. 2006. Biomechanics of single zonal chondrocytes. *J. Biomech.* 39:1595–1602.

51. Li, Y. S. 2014. Study on the mechanical models for micropipette aspiration of cells. Ph D thesis. Taiyuan University of Technology, In Chinese.

52. Boudou, T., J. Ohayon, …, P. Tracqui. 2006. An extended modeling of the micropipette aspiration experiment for the characterization of the Young's modulus and Poisson's ratio of adherent thin biological samples: numerical and experimental studies. *J. Biomech.* 39:1677–1685.

53. Darling, E. M., M. Topel, …, F. Guilak. 2008. Viscoelastic properties of human mesenchymally-derived stem cells and primary osteoblasts, chondrocytes, and adipocytes. *J. Biomech.* 41:454–464.

54. Koay, E. J., A. C. Shieh, and K. A. Athanasiou. 2003. Creep indentation of single cells. *J. Biomech. Eng.* 125:334–341.

55. Zhang, Q. Y. 2006. Mechanical properties of chondrocytes from normal and osteoarthritic rabbit knee cartilage. Master thesis. Taiyuan University of Technology, In Chinese.